Carbohydrate Polymers 83 (2011) 447–451

Contents lists available at ScienceDirect

Carbohydrate Polymers

journal homepage: www.elsevier.com/locate/carbpol

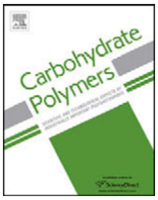

Effect of carboxylate multi-walled carbon nanotubes on the performance of thermoplastic starch nanocomposites

Liu Zhanjun[a,b], Zhao Lei[c], Chen Minnan[c], Yu Jiugao[a,*]

[a] School of Science, Tianjin University, Tianjin 300072, China
[b] Department of Pharmaceutics, North China Coal Medical University, Tangshan 063000, China
[c] College of Material Science and Chemical Engineering, Tianjin Polytechnic University, Tianjin Tianjin 300160, China

ARTICLE INFO

Article history:
Received 15 July 2010
Received in revised form 29 July 2010
Accepted 2 August 2010
Available online 11 August 2010

Keywords:
Carboxylate multi-walled carbon nanotubes
Nanocomposites
Thermoplastic
Starch

ABSTRACT

A facile solution dispersion method is used to prepare high performance thermoplastic starch (TPS)/carboxylate multi-walled carbon nanotubes (CMWNTs) nanocomposites. Transmission electron microscopy demonstrates glycerol pretreatment can further restrain the agglomeration of CMWNTs. So the improved dispersion and hydrophilicity of CMWNTs are favorable to enhance the compatibility and homogeneity of TPS/CMWNTs nanocomposites. The improvements of CMWNTs content enhance both the pasting viscosity of cornstarch and thermal stability of TPS matrix proved by rapid visco analysis and thermogravimetric analysis, respectively. Scanning electron microscopy reveals that homogeneous TPS/CMWNTs nanocomposites can be achieved when CMWNTs content is below 1.5 wt%. CMWNTs can also form a perfect electric conductive network in TPS matrix at this concentration. However, higher CMWNTs content deteriorate the plasticization of cornstarch detected by Fourier transform infrared. Therefore, mechanical test shows that the residue cornstarch granules influence the load transfer from TPS matrix to the ultra-strong carbon nanotubes (CNTs).

1. Introduction

Polymer nanocomposites offer a wide range of promising applications because of their much enhanced properties arising from the reinforcement of nanoparticles (Zeng, Yu, & Lu, 2008). Compared to conventional composites, polymer nanocomposites maximize the polymer–nanoparticle interactions, since the filler is dispersed on a nanometer scale. This results in lighter materials with higher performance, rendering them desirable for many applications. Carbon nanotubes (CNTs) have gained a high interest, moreover, a constantly expanding number of studies can be found in the literature concerning their uses, properties and applications based on many polymers composites (Coleman, Khan, Blau, & Gun'ko, 2006; Thostenson, Ren, & Chou, 2001).

CNTs have received much attention since their discovery by Iijima (1991). Two main types of CNTs exist: single-walled carbon nanotubes (SWCNTs) and multi-walled carbon nanotubes (MWCNTs). However, strong van der Waals interactions among pristine CNTs result in their bundling and aggregation, preventing their facile individualization. On the other hand, CNTs maintain notoriously poor solubility in aqueous media as well as in organic solvents. Therefore, the dispersion of CNTs should be very fine in polymer matrix, which means that the interfacial interaction between CNTs and the matrix should be optimized. To solve this problem, both covalent and non-covalent functional modifications of CNTs have been widely studied based on different polymer matrix (Chen et al., 2002; Coleman et al., 2006; Peng & Wong, 2009).

Starch is one of the most plentiful natural biopolymers, which composes mainly of amylose (poly-α-1,4-D-glucan) and amylopectin (poly-α-1,4-D-glucan and α-1,6-D-glucan). In addition to being staple food, starch has recently gained interest as a renewable and biodegradable plastic. In the presence of plasticizer, thermoplastic starch (TPS) can be prepared by solution casting or melt extrusion processing (Averous, 2004). Recently electro-active polymer based on TPS has aroused a great deal of interest. Both ionic liquid (Wang, Zhang, & Wang, 2009) and N,N-dimethylacetamide combined with lithium chloride (Wang, Zhang, Liu, & Wang, 2009) have been used as novel plasticizers to enhance the ionic conductivity of TPS. Moreover, amylose chain has been found can wrap around the SWCNTs, the inner core of the helix being filled by SWCNTs (Kim et al., 2003; Star, Steuerman, Heath, & Stoddart, 2002). This method can be used for the homogeneous dispersion of SWCNTs in water. At the same time, Tomasik et al. (Stobinski et al., 2003) also suggest that small SWCNTs can be enveloped by amylose to form a nano-shock-absorber. They also point out interactions of SWCNTs with waxy corn amylopectin are stronger than with potato amylopectin (Lii, Stobinski, Tomasik, & Liao, 2003). The success in dispersion of CNTs in solution will greatly benefit to prepare various polymer/CNTs composites by solution casting method.

---

* Corresponding author. Tel.: +86 22 27406144; fax: +86 22 27403475.
E-mail address: gaojiuy@gmail.com (J. Yu).

0144-8617/$ – see front matter © 2010 Elsevier Ltd. All rights reserved.
doi:10.1016/j.carbpol.2010.08.007

Compared with SWCNTs, MWCNTs is low price and abundant enough. Moreover, MWCNTs have been proven to be very effective filler at very low loadings. This is because neat MWCNTs exhibit high aspect ratio (as high as 1000), excellent mechanical (as high as 1 TPa tensile modulus), thermal, and electrical properties (Curran et al., 1998). Ma, Yu, and Wang (2008) have used sodium dodecylsulfate as surfactant for MWCNTs to prepare glycerol plasticized-starch/MWCNTs composites. They point out that MWCNTs not only enhance the mechanical property of this composite, but also endows electrical conductivity. However, the huge out diameter (compared with SWCNTs) and smooth surface of MWCNTs deteriorate compatibility in this complex composite.

In order to achieve TPS/MWCNTs with high performance, a flexible way is to introduce hydrophilic groups on the surface of MWCNTs. Carboxylate MWCNTs (CMWNTs) is the simplest covalent functional modification CNTs. Carboxylic acid groups can be introduced onto the tips and defect sites of CNTs surfaces by refluxing in a mixture of concentrated sulfuric acid and nitric acid (Kuznetsova et al., 2000; Wang, Qu, Guo, Li, & Liu, 2006). The improvement of water dissolve ability will favor CMWNTs dispersion in TPS, since starch contains hydroxide groups, hydrogen-bonding between CMWNTs and starch is potentially achievable and should improve the interfacial interaction as well as the nanocomposites performance. So TPS/CMWNTs nanocomposites with CMWNTs contents ranged from 0.5 to 3.0 wt% are prepared by solution casting in this paper. The effects of CMWNTs content on the structure and properties of the nanocomposites are investigated by transmission electron microscopy (TEM), rapid visco analyser (RVA), scanning electron microscopy (SEM), Fourier transform infrared (FT-IR), thermogravimetric analysis, mechanical and electric conductivity testing.

2. Experimental

2.1. Materials

CMWNTs were purchased from Institute of Organic Chemistry in Chengdu of Chinese Academy of Sciences (Chengdu, China). They were prepared by oxidative acid treatment of MWCNTs (produced by the arc-discharge method). Carboxylic group concentration was about 2 wt% according to the product description and our testing. Cornstarch (12 wt% moisture) was obtained from Langfang Starch Company (Langfang, Hebei, China). Glycerol (analytical reagent) was purchased from Tianjin Chemical Reagent Factory (Tianjin, China).

2.2. Preparation of TPS/CMWNTs nanocomposites

CMWNTs were dispersed in a solution of distilled water (100 ml) containing glycerol (1.5 g) and ultrasonicated for 30 min before adding 5 g cornstarch. The CMWNTs loading level was 0, 0.5, 1.0, 1.5, 2.0, and 3.0 wt% based on the amount of cornstarch, respectively. The mixture was heated at 95 °C for 30 min with constant stirring in order to plasticize cornstarch. The obtained solution was cast onto a polystyrene tray, with the length of 20 cm and the width of 15 cm. Then the mixtures were placed in an air-circulating oven at 60 °C until dry (about 6–8 h). The obtained films with the thickness of 0.5 mm were preconditioned in a climate chamber at 20 °C and 50% RH for at least 48 h prior to all testing.

2.3. Characterization

Transmission electron microscopy (TEM) and a field emission scanning electron microscopy (SEM) were used to characterize the micro-structure of CMWNTs and its nanocomposites, respectively. TEM was performed with a JEM-1200EX microscope (JEOL, Tokyo, Japan), operating at an accelerating voltage of 80 kV. SEM was performed with a JEOL JSM 6700F (JEOL, Tokyo, Japan). Both the fracture faces (samples were cooled in liquid nitrogen, then broken) and failure surfaces (after tensile tests) were coated with gold under vacuum for SEM observation.

The pasting property was analyzed using a rapid viscoanalyser (Newport Scientific, Sydney, Australia) according to AACC method 76-21 (Xie & Liu, 2004). CMWNTs were dispersed into a solution of distilled water (25 ml) and glycerol (0.375 g) then ultrasonicated for 30 min before adding 1.25 g cornstarch. The obtained starch slurry had the same composition as the mixture used for casting the TPS/CMWNTs nanocomposites. The starch slurry was held at 50 °C for 1 min, then heated to 95 °C at 12.2 °C/min and held at 95 °C for 2.5 min. It was then cooled to 50 °C (cooling rate of 11.8 °C/min) and held at 50 °C for 2 min. The paddle speed was 960 rpm for 10 s and then decreased to 160 rpm for the remainder of the experiment.

TGA was carried out on STA409PC thermal analysis instrument (Netzsch, Germany). TPS, CMWNTs and their nanocomposites were cut into small pieces. The samples were about 5–10 mg in a sealed aluminum pan; the range of testing temperature was from room temperature to 450 °C at a heating rate of 10 °C/min.

Fourier transform infrared (FT-IR) spectroscopy was obtained at 2 cm^{-1} resolution with BIO-RAD FTS3000 IR Spectrum Scanner (Hercules, USA). Typically, 64 scans were signal-averaged to reduce spectral noise. The samples were compressed to the sheet with the thickness of about 0.5 mm in the Flat Sulfuration Machine, tested by attenuated total reflection measurements.

According to the GB1040-79 standard of China, the tensile strength and elongation at break of nanocomposites were measured using a Testometric AXM350-10KN materials testing machine (Rochdale, Lancashire, UK). The crosshead speed was 50 mm/min. All samples were tested after being stored in an air-tight container for 1 week after preparation. Each measurement was performed for five specimens and averaged.

Volume resistivity measurements were performed on samples of all composites that were compressed into thin sheets. A Model ZC36 electrometer (SPSIC Huguang Instruments & Power Supply Branch, China) was used for high resistivity samples with 50 mm diameter and 0.5 mm thickness. For more conductive samples (larger than 10^6 S/cm) strips with dimensions of 30 mm × 5 mm and 0.5 mm thickness were measured using a Model ZL7 electrometer (SPSIC Huguang Instruments & Power Supply Branch, China) using a four-point test fixture.

3. Results and discussion

Fig. 1a shows the TEM image of CMWNTs (dispersed in a solution of distilled water and ultrasonicated for 30 min). The CMWNTs were curved and coiled. Due to their huge surface area, CMWNTs tangled together but could be identified. They were central hollow tubes in the center, with 5–10 nm in internal diameter, 10–20 nm in external diameter, 0.5–500 μm in length, and 10–30 graphite layers. CMWNTs were partially oxidized via acid treatment and had carboxyl functionalities and double bond in the open ends, sidewalls and defect sites, similar as previous report (Wang et al., 2006). Fig. 1b shows the TEM image of CMWNTs treated with glycerol solution (dispersed in glycerol solution and ultrasonicated for 30 min) to study the dispersion effect of glycerol on CMWNTs. Compared with water, glycerol containing much hydroxyl groups could dramatically increase the dispersion of CMWNTs in water solution and restrain the agglomeration of CMWNTs. Therefore, the better dispersion of CMWNTs would greatly benefit to prepare high performance TPS/CMWNTs nanocomposites by solution casting.

The viscosity of cornstarch paste was a very important parameter for preparing TPS/CMWNTs nanocomposites by solution

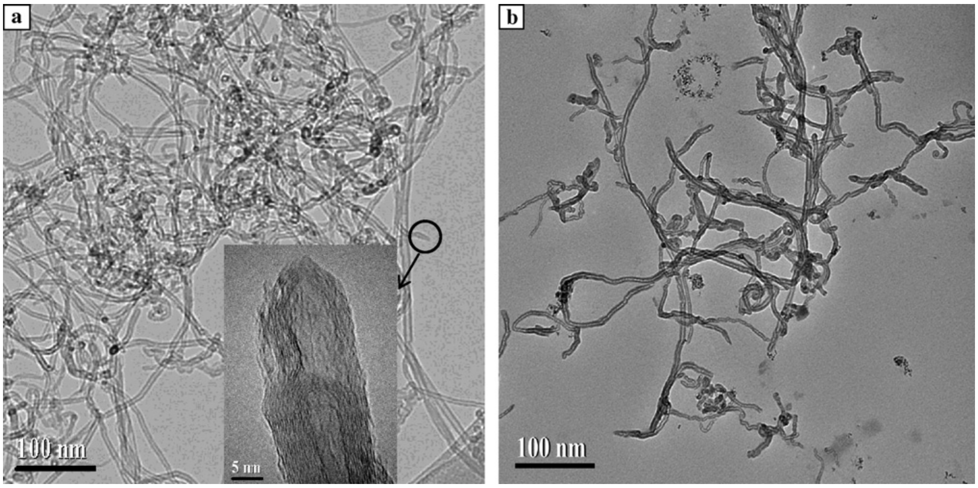

Fig. 1. TEM micrograph for CMWNTs dispersed in water solution (a) and CMWNTs dispersed in glycerol solution (b).

casting. Therefore, the effect of CMWNTs content on the pasting properties of cornstarch was studied by the RAV. In order to simulate the processing of TPS/CMWNTs nanocomposites, the composition of the slurry identical to the casting solution was used in RVA analysis. When granular cornstarch began to gelatinize in water, the viscosity increased as well as cornstarch slurry turned into paste. At the same time, the improvement of CMWNTs content could obviously increase the pasting viscosity of the paste as shown in Fig. 2. Except to the high aspect ratio of CMWNTs, it might be related to the intense hydrogen bond interaction between the carboxylic acid groups of CMWNTs and polyhydroxy cornstarch.

Moreover, CMWNTs not only could improve the pasting viscosity of this composite, but also increased the thermal stability of TPS matrix. Thermogravimetric curves were performed to detect the thermal stability of TPS and TPS/CMWNTs nanocomposites in the temperature range from 25 to 450 °C. As shown in Fig. 3, the first step decomposition of TPS and TPS/CMWNTs nanocomposites was about 100 °C mainly ascribed to the water evaporation. Moreover, the second step was related to glycerol and starch decomposition (Wang, Yu, Chang, & Ma, 2008). When the section 260–315 °C of thermogravimetric curves was enlarged in Fig. 3, it could be found the weight loss of nanocomposites decreased with increasing CMWNTs content clearly. Compared with TPS, the CMWNTs was more stable. It displayed weight loss of 2 wt% on the whole weight loss process (as shown in Fig. 3), which was assigned to the decomposition of free carboxyl groups on the surface of CMWNTs. The stabilization effect of CMWNTs on thermal stability of the composites could be explained that a barrier effect of the nanotubes and their formed aggregates hindered the diffusion of the degradation products from the bulk of the polymer onto the gas phase (Chatterjee & Deopura, 2006; Yang et al., 2005). Furthermore, carboxyl groups on the surface of CMWNTs could increase interfacial interactions between CMWNTs and TPS matrix, which improved the degradation's activation energy.

Dispersion of CMWNTs in TPS matrix was one of the key elements to the mechanical properties and electrical conductivity of TPS/CMWNTs nanocomposites. Fig. 4a and b shows the fracture surfaces of TPS/1.5 wt% CMWNTs (brittle fracture in liquid nitrogen) and TPS/3.0 wt% CMWNTs (after tensile testing) nanocomposites, respectively. As shown in Fig. 4a, the well-dispersed bright dots and lines were the ends of CMWNTs. SEM image clearly showed a homogeneous dispersion of CMWNTs throughout the TPS matrix at lower CMWNTs loading (below 1.5 wt%). At the same time, TPS presented a continuous phase and no residue cornstarch granules could be detected after solution casting. However, upon failure, the fracture surface of the composites containing 3.0 wt% CMWNTs was poor as shown in Fig. 4b. Most cornstarch granules were only partly destroyed and embedded in a partially plasticized-starch matrix. This phenomenon indicated higher CMWNTs loading could deteriorate the plasticization of cornstarch. This result could be also

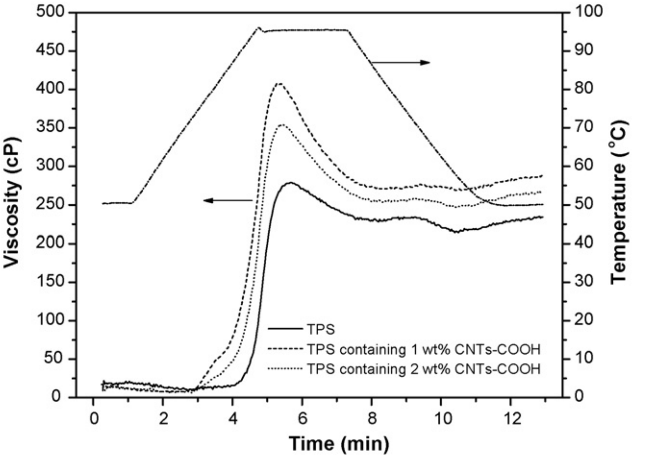

Fig. 2. Effect of CMWNTs content on the viscometric profile.

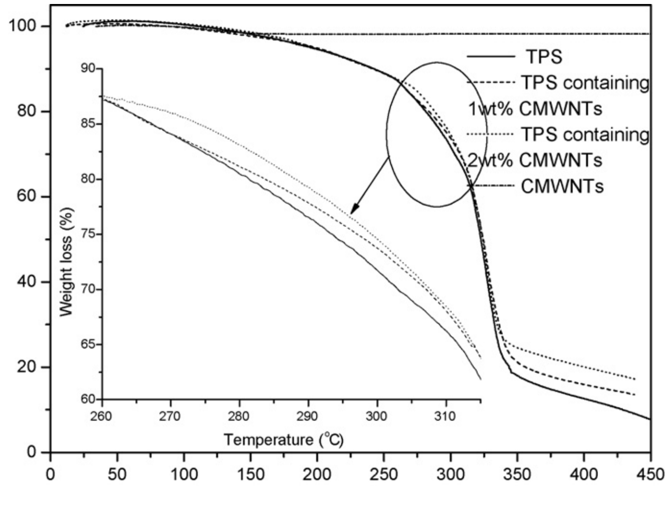

Fig. 3. Thermogravimetric curves of TPS, CMWNTs and TPS/CMWNTs nanocomposites.

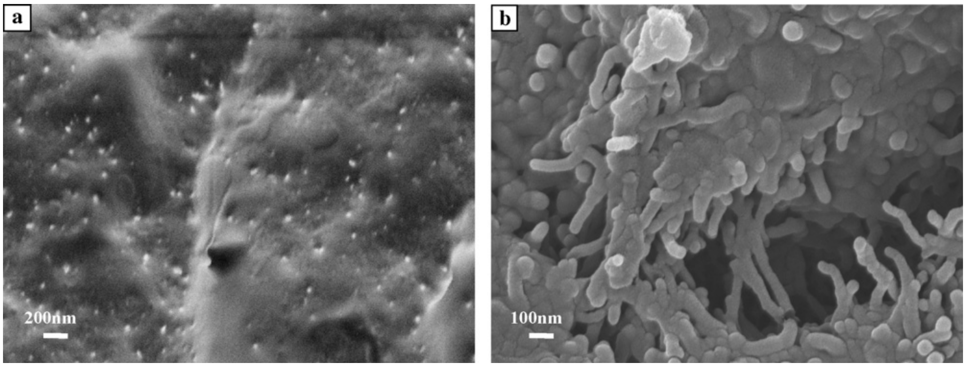

Fig. 4. SEM images of the fracture (a) and failure surfaces (b) for TPS/CMWNTs films.

confirmed by FT-IR analysis. Moreover, it was worth noting that most of the CMWNTs were just pulled out of TPS matrix rather than broken. At the same time, compared with pristine CMWNTs (as shown in Fig. 1a), the diameter of the pulled out CMWNTs became bigger, achieved to 50 nm. It seemed to be well wrapped or encapsulated by the TPS matrix. Therefore, this suggested good interfacial adhesion existed between TPS and CMWNTs.

FT-IR analysis of the TPS based composites could identify the plasticization of starch (Wang et al., 2008). On the basis of the harmonic oscillator model, it concluded that the lower the peak frequency the higher was the plasticization of TPS (Pawlak & Mucha, 2003). Fig. 5 shows the FT-IR spectrum of TPS and TPS/CMWNTs nanocomposites, respectively. In the fingerprint region of FT-IR spectrum of TPS, three characteristic peaks appeared between 1200 and 900 cm^{-1}, attributed to C–O bond stretching of starch (Fang, Fowler, Tomkinson, & Hill, 2002). The characteristic peaks of native cornstarch (the –C–O– bond stretching of the –C–O–H group at about 1156 and 1081 cm^{-1} and the –C–O– bond stretching of the –C–O–C– group in the anhydroglucose ring at about 1020 cm^{-1}; Fang et al., 2002) shifted to lower wavenumbers in TPS as shown in Fig. 5. Moreover, the single peak at about 1020 cm^{-1} changed to double peak after plasticized by glycerol. Compared with TPS, the corresponding characteristic peaks of TPS/CMWNTs nanocomposites shifted to higher wavenumber. Especially, TPS/3.0 wt% CMWNTs nanocomposites showed the highest wavenumber. It indicated that high CMWNTs content could deteriorate the plasticization of cornstarch. Moreover, the poor plasticization of cornstarch destructed the efficient load transfer from TPS matrix to the ultra-strong CNTs fillers. This result could be also confirmed by tensile testing.

The mechanical properties of TPS were very poor as previous report (Wang, Zhang, Han, & Bai, 2009). So it was necessary to reinforce the TPS matrix with the nanofiller. Fig. 6 shows the tensile properties of TPS/CMWNTs nanocomposites with different CMWNTs contents, which were tested after being stored in a climate chamber at 20 °C and 50% RH for 48 h. It could be found that the addition of CMWNTs significantly improved the tensile strength of TPS matrix as CMWNTs loading below 1.5 wt%, but just the reverse for elongation at break. As the CMWNTs content increased to 1.5 wt%, the tensile strength of TPS/CMWNTs nanocomposites could achieve to 7.7 MPa, while the pure TPS was only 4.5 MPa. Because acid-treatment process incorporated kinds of polar groups with MWCNTs, improved the hydrophilicity of MWCNTs, and reduced agglomerations of MWCNTs (Wang et al., 2006). Therefore, CMWNTs were greatly benefited to enhance the hydrogen-bonding interactions as well as the dispersion in TPS/CMWNTs nanocomposites, and result in an improvement of the mechanical performance of the TPS/CMWNTs nanocomposite films. However, the high content CMWNTs (above 1.5 wt%) could not only deteriorate the plasticization of TPS, but also destructed the continuity of TPS matrix. Therefore, higher CMWNTs contents (above 1.5 wt%) could deteriorate the mechanical properties of TPS/CMWNTs.

Fig. 7 shows the electrical conductivity of TPS/CMWNTs nanocomposites measured at room temperature to investigate the effect of CMWNTs content on electrical conductivity. For an elec-

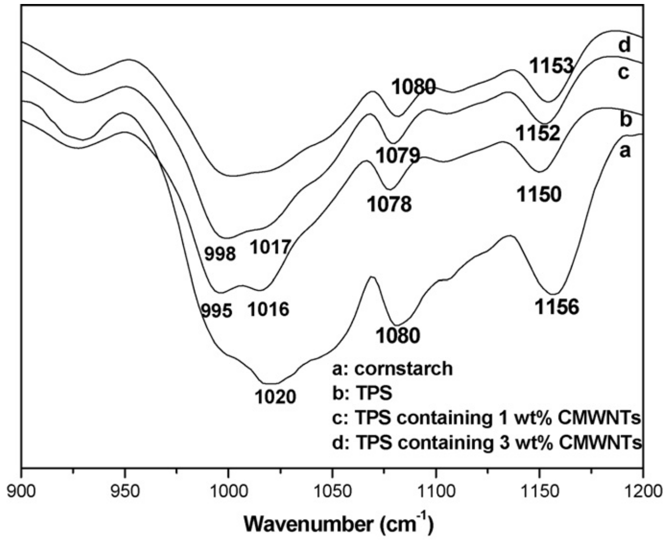

Fig. 5. FT-IR spectra of TPS and TPS/CMWNTs films.

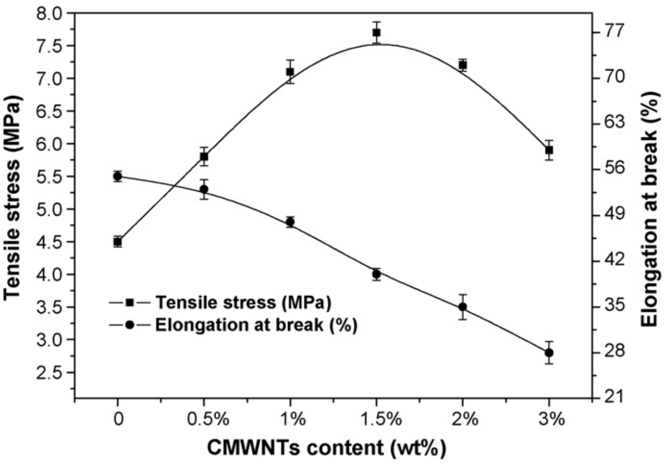

Fig. 6. The effect of CMWNTs contents on mechanical properties of TPS/CMWNTs nanocomposites.

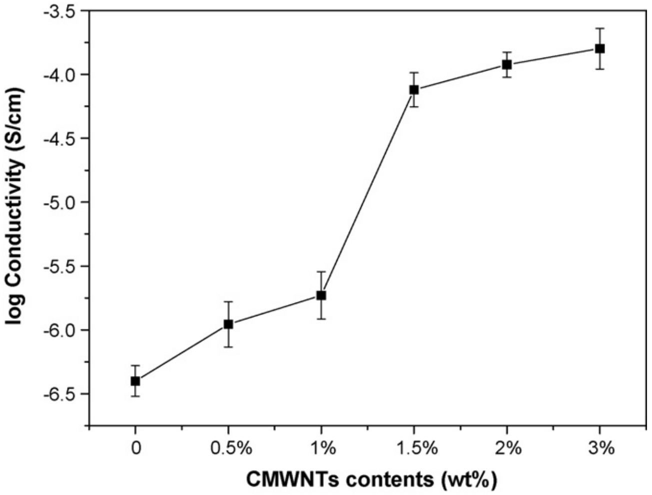

Fig. 7. The electrical conductivity of TPS with deferent CMWNTs content.

tric conductive network to be formed, CNTs do not require real overlap with each other, since a conductive network can be formed through hopping and tunneling processes (Lee, Cho, Jeon, & Youn, 2007). Therefore, there was a pronounced increase in conductivity at the CMWNT content of 1.5 wt%, where it was assumed that the network was formed by geometrical overlapped CMWNTs. This indicated that the glycerol solution pretreatment CMWNTs was benefit to generate a well-dispersed TPS/CMWNTs nanocomposite. Moreover, threshold value for percolation could be further lowered with improved dispersion of CMWNTs in TPS matrix.

4. Conclusion

This paper mainly reported the high performance TPS/CMWNTs nanocomposites based on renewable source. Glycerol could further increase the dispersion of acidified CMWNTs in water solution. The improved dispersion and compatibility were benefit to increase the interfacial interaction as well as the properties of the composites. Therefore, homogeneous TPS/CMWNTs nanocomposites could be achieved by solution casting. Moreover, CMWNTs could improve the pasting viscosity of cornstarch and thermal stability of TPS matrix. TPS/CMWNTs nanocomposites also exhibited the electrical percolation thresholds of 1.5 wt% CMWNTs. More CMWNTs had no obvious improvement for the conductivity, moreover, could deteriorate the plasticization of TPS and the mechanical properties of the composites.

References

Averous, L. (2004). Biodegradable multiphase systems based on plasticized starch: A review. *Journal of Macromolecular Science-Polymer Reviews*, *C44*(3), 231–274.

Chatterjee, A., & Deopura, B. L. (2006). Thermal stability of polypropylene/carbon nanofiber composite. *Journal of Applied Polymer Science*, *100*(5), 3574–3578.

Chen, J., Liu, H. Y., Weimer, W. A., Halls, M. D., Waldeck, D. H., & Walker, G. C. (2002). Noncovalent engineering of carbon nanotube surfaces by rigid, functional conjugated polymers. *Journal of the American Chemical Society*, *124*(31), 9034–9035.

Coleman, J. N, Khan, U., Blau, W. J., & Gun'ko, Y. K. (2006). Small but strong: A review of the mechanical properties of carbon nanotube–polymer composites. *Carbon*, *44*(9), 1624–1652.

Curran, S. A., Ajayan, P. M., Blau, W. J., Carroll, D. L., Coleman, J. N., Dalton, A. B., et al. (1998). A composite from poly(m-phenylenevinylene-co-2,5-dioctoxy-p-phenylenevinylene) and carbon nanotubes: A novel material for molecular optoelectronics. *Advanced Materials*, *10*(14), 1091–1093.

Fang, J. M., Fowler, P. A., Tomkinson, J., & Hill, C. A. S. (2002). The preparation and characterisation of a series of chemically modified potato starches. *Carbohydrate Polymers*, *47*(3), 245–252.

Iijima, S. (1991). Helical microtubules of graphitic carbon. *Nature*, *354*(6348), 56–58.

Kim, O. K, Je, J. T., Baldwin, J. W., Kooi, S., Pehrsson, P. E., & Buckley, L. J. (2003). Solubilization of single-wall carbon nanotubes by supramolecular encapsulation of helical amylose. *Journal of the American Chemical Society*, *125*(15), 4426–4427.

Kuznetsova, A., Mawhinney, D. B., Naumenko, V., Yates, J. T., Liu, J., & Smalley, R. E. (2000). Enhancement of adsorption inside of single-walled nanotubes: Opening the entry ports. *Chemical Physics Letters*, *321*(3–4), 292–296.

Lee, S. H., Cho, E., Jeon, S. H., & Youn, J. R. (2007). Rheological and electrical properties of polypropylene composites containing functionalized multi-walled carbon nanotubes and compatibilizers. *Carbon*, *45*(14), 2810–2822.

Lii, C. Y., Stobinski, L., Tomasik, P., & Liao, C. D. (2003). Single-walled carbon nanotube—potato amylose complex. *Carbohydrate Polymers*, *51*(1), 93–98.

Ma, X. F., Yu, J. G., & Wang, N. (2008). Glycerol plasticized-starch/multiwall carbon nanotube composites for electroactive polymers. *Composites Science and Technology*, *68*(1), 268–273.

Pawlak, A., & Mucha, A. (2003). Thermogravimetric and FTIR studies of chitosan blends. *Thermochimica Acta*, *396*(1–2), 153–166.

Peng, X. H., & Wong, S. S. (2009). Functional covalent chemistry of carbon nanotube surfaces. *Advanced Materials*, *21*(6), 625–642.

Star, A., Steuerman, D. W., Heath, J. R., & Stoddart, J. F. (2002). Starched carbon nanotubes. *Angewandte Chemie-International Edition*, *41*(14), 2618–2622.

Stobinski, L., Tomasik, P., Lii, C. Y., Chan, H. H., Lin, H. M., Liu, H. L., et al. (2003). Single-walled carbon nanotube—amylopectin complexes. *Carbohydrate Polymers*, *51*(3), 311–316.

Thostenson, E. T., Ren, Z. F., & Chou, T. W. (2001). Advances in the science and technology of carbon nanotubes and their composites: A review. *Composites Science and Technology*, *61*(13), 1899–1912.

Wang, G. J., Qu, Z. H., Guo, J. L., Li, Y., & Liu, L. (2006). Study of multiple-wall carbon nanotubes functionalized by the poly(styrene-co-maleic anhydride). *Acta Chimica Sinica*, *64*(24), 2505–2508.

Wang, N., Yu, J. G., Chang, P. R., & Ma, X. F. (2008). Influence of formamide and water on the properties of thermoplastic starch/poly(lactic acid) blends. *Carbohydrate Polymers*, *71*(1), 109–118.

Wang, N., Zhang, X. X., Han, N., & Bai, S. H. (2009). Effect of citric acid and processing on the performance of thermoplastic starch/montmorillonite nanocomposites. *Carbohydrate Polymers*, *76*(1), 68–73.

Wang, N., Zhang, X. X., Liu, H. H., & Wang, J. P. (2009). N,N-Dimethylacetamide/lithium chloride plasticized starch as solid biopolymer electrolytes. *Carbohydrate Polymers*, *77*(3), 607–611.

Wang, N., Zhang, X. X., & Wang, X. C. (2009). Ionic liquids modified montmorillonite/thermoplastic starch nanocomposites as ionic conducting biopolymer. *Macromolecular Research*, *17*(5), 285–288.

Xie, X. J., & Liu, Q. (2004). Development and physicochemical characterization of new resistant citrate starch from different corn starches. *Starch-Starke*, *56*(8), 364–370.

Yang, J., Lin, Y. H., Wang, J. F., Lai, M. F., Li, J., Liu, J. J., et al. (2005). Morphology, thermal stability, and dynamic mechanical properties of atactic polypropylene/carbon nanotube composites. *Journal of Applied Polymer Science*, *98*(3), 1087–1091.

Zeng, Q. H, Yu, A. B., & Lu, G. Q. (2008). Multiscale modeling and simulation of polymer nanocomposites. *Progress in Polymer Science*, *33*(2), 191–269.